remote sensing

MDPI

Article

Identifying the Coupling Coordination Relationship between Urbanization and Ecosystem Services Supply–Demand and Its Driving Forces: Case Study in Shaanxi Province, China

Jiamin Liu, Hao Wang *, Le Hui, Butian Tang, Liwei Zhang and Lei Jiao

School of Geography and Tourism, Shaanxi Normal University, Xi'an 710119, China; liujiamin@snnu.edu.cn (J.L.); 2002huile@snnu.edu.cn (L.H.); tangbutian@snnu.edu.cn (B.T.); zlw@snnu.edu.cn (L.Z.); ljiao@snnu.edu.cn (L.J.)
* Correspondence: foreva@snnu.edu.cn

Abstract: Exploring the relationship and driving forces between supply–demand of ecosystem services (ESs) and urbanization can help solve the environmental problems and promote regional sustainable development. This study analyzed the spatio-temporal distribution characteristics of supply–demand of ESs and comprehensive urbanization level (CUL) in Shaanxi Province from 2010 to 2019 and assessed the coupling relationship between ecosystem service supply–demand ratio (ESSDR) and CUL using the coupling coordination degree (CCD) model. Random forests and geographically weighted regression methods were utilized to characterize the contribution and spatial distribution of the drivers of CCD. The results showed that: (1) except for habitat quality, the ESSDR of the other three types of services as well as the comprehensive services showed a decreasing trend, CUL exhibited increasing trend; (2) Although CCD was generally increasing, a significant portion (78.51%) of regions still remained uncoordinated, with relatively better coordination shown around the Guanzhong urban agglomeration, which has a higher urbanization level; (3) The CCD in Shaanxi Province was primarily influenced by local financial income, the secondary industry, and temperature forces. In regions with high and increasing CCD, the tertiary industry was the decisive force. In other areas, there were significant spatial variations in the driving forces. These findings provide a coupled and coordinated perspective for urban ecological management, which can provide scientific reference and practical guidance for cities with different development modes.

Keywords: urbanization; supply and demand; coupling coordination degree; geographically weighted regression; random forest

check for updates

Citation: Liu, J.; Wang, H.; Hui, L.; Tang, B.; Zhang, L.; Jiao, L. Identifying the Coupling Coordination Relationship between Urbanization and Ecosystem Services Supply–Demand and Its Driving Forces: Case Study in Shaanxi Province, China. *Remote Sens.* **2024**, *16*, 2383. https://doi.org/10.3390/rs16132383

Academic Editor: Jeroen Meersmans

Received: 4 June 2024
Revised: 25 June 2024
Accepted: 26 June 2024
Published: 28 June 2024

Copyright: © 2024 by the authors. Licensee MDPI, Basel, Switzerland. This article is an open access article distributed under the terms and conditions of the Creative Commons Attribution (CC BY) license (https://creativecommons.org/licenses/by/4.0/).

1. Introduction

Ecosystem services (ESs) serve as a pivotal connection between ecosystem structures, processes, functions, and the needs and well-being of social systems. They are instrumental in delineating socio-ecosystem interactions and facilitating effective ecological management [1,2]. ES supply is defined as the essential raw materials and services offered by ecosystems for human production and survival, and demand encompasses the human utilization and consumption of these raw materials and ecosystem-generated products, thus constituting the dynamic mechanism of ecosystem service flow from natural ecology to human society [3,4]. The supply–demand relationship of ES is an external characterization of the complex material and energy flows and interactions in the ecological–social–economic complex system, reflecting the spatial allocation of ecological resources and the coordination of socio-economic subsystems [5,6]. The investigation of supply–demand relationships has emerged as a prominent field of study, with rapid advancements in quantitative research methodologies [7,8]. The scale of research has expanded from small and medium scales such as streets, watersheds, mountains, and basins to national and global scales [9–11]. For example, Ghasemi used a wide range of indicators to map and assess the northern Iranian NbR supply and demand [12]; Quanyi Liu quantified the spatial gradient of ES supply and

demand in six cities of Danjiangkou Basin, Hubei Province, using an improved sigmoid function [13]. Studying ESs from a supply–demand viewpoint and addressing mismatches between them are essential for ecological security and sustainable development.

Currently, rapid urbanization and unreasonable socio-economic activities have increased the interference and pressure on ecosystems. At the beginning of the 21st century, about 60% of the 24 global ESs were in a state of decline or unsustainable development [14], resulting in the destruction of ecosystems' original functional structure and ecological processes, and diminishing of ES supply capacity [15,16]. As socio-economic levels progress, increasing demands for enhanced quality of life have led to a heightened demand for services like climate regulation, water yield, and soil retention, which are critical to maintaining a sustainable environment. The decline in ES supply capacity and the growth in human well-being demand led to quantitative imbalances and spatial discrepancies between supply and demand [17], and triggered a number of ecological risks [18]. The imbalance between supply and demand has obstructed high-quality sustainable development, profoundly affecting both ecological security and regional sustainability [19,20].

To achieve the coordinated development of urbanization and the natural environment, it is imperative to enhance our comprehension and management of the interplay between ES supply–demand and urbanization [21,22]. Numerous researches have evaluated the effects of urbanization on the supply–demand of ESs [23,24]. These studies have demonstrated that urbanization significantly impacts the supply and demand of ESs at various scales [25,26]. However, the relationship between urbanization and the ecological environment is characterized by a nonlinear and interactively coupled dynamic [27]. A robust ecological environment underpins human survival and sustainable urban development, while high-quality urbanization contributes technical and financial resources to improve ecosystem [28,29]. The coupling coordination model is suitable for the analysis of intricate systems comprising multiple interacting indicators and dimensions [30], which can effectively quantify the nonlinear correlation between urbanization and ecosystems [31]. Understanding the intricate interplay between urbanization and the environment, and evaluating whether these interactions are harmonious or conflicting, is crucial for reaching a harmony between the progress of urban development and the preservation of ecosystem.

Furthermore, although many studies have explored how urbanization influences the supply–demand relationship of ESs, there remains a gap in comprehensively understanding the internal mechanisms of this coupling relationship [32]. Current mechanism analyses are mostly driven by mathematical and statistical models such as Geo detector [33], correlation analysis [34], and redundancy analysis [35,36]. These approaches, however, disregarded spatial variability within regional contextual variations, yielding merely numerical outputs that fail to capture spatial variability in the driving forces or to provide targeted and practical recommendations for ecosystem management [37,38]. With advancements in underlying theories and methodologies, models such as geographically weighted regression (GWR) have emerged as effective tools for analyzing the spatial heterogeneity of impact forces at coupled scales [39,40]. Additionally, although some researchers have explored various forces that influence the dependent variable, the relative importance of these forces often remains undetermined. The random forest (RF) approach stands out in this context, provides a robust methodology for evaluating the significance of variables, clarifying the contributions of various influencing forces, and addressing the limitations of traditional analytical methods [41,42].

Shaanxi Province is recognized as the most economically active and ecologically complex region in Northwest China. The intensified human activities driven by urbanization, and the spatial imbalance between natural resource endowment and socio-economic development, have sharpened the supply–demand conflicts of ESs, posing a crucial challenge to the pursuit of high-quality sustainable development. This paper analyzes supply–demand changes of four key ESs from 2010 to 2019, adopts the Coupling Coordination Degree (CCD) model to explore the coupling relationship between Comprehensive Urbanization Level (CUL) and the Ecosystem Service Supply–Demand Ratio (ESSDR), and utilizes Geograph-

ically Weighted Regression (GWR) and Random Forest (RF) methodologies to identify forces influencing this relationship. The following are the study's primary goals: (1) to investigate the spatial characteristics of the supply–demand changes of ESs; (2) to reveal CCD between CUL and ESSDR; and (3) to investigate and quantify the forces affecting the CCD. The research findings are anticipated to offer valuable insights that will support decision-making in urban planning and ecological management across the region.

2. Data and Methods

2.1. Study Area

Shaanxi Province is situated in the west-central region of China, covers an area of 205,624 km^2, and is governed by 10 prefectural-level cities, 31 municipal districts, 7 county-level cities, and 69 counties (Figure S1, Table S1). Its longitudes range from 105°29′ to 111°15′ E, and it latitudes from 31°42′ to 39°35′ N. The terrain of Shaanxi is low in the middle and high in the north and south, with a variety of landform types, spanning the Loess Plateau, the Guanzhong Plain, and the Qinba Mountains from north to south. It is thus split into the northern Shaanxi, Guanzhong, and southern Shaanxi regions (Figure 1). The northern Shaanxi region is rich in coal resources, but the ecological environment is fragile. The Guanzhong Plain region has a flat terrain, convenient transportation, and rapid economic development. Southern Shaanxi is an important ecological reserve in China, but the level of economic development is low. Shaanxi Province has a diverse geographic environment containing plains, hills, and mountains, and the resource endowment of different regions varies significantly. Studying the impact of different natural resources and geographic environments on economic development can provide a scientific basis for the formulation of regional development policies. The implementation of national development strategies such as "Western Development" and "the Belt and Road" has created new opportunities and challenges for the balanced development of urbanization and the ecological environment in Shaanxi. The population of Shaanxi Province has experienced a consistent increase, while urbanization level has been steadily rising, so the contradiction between the ecological environment and the urban development has become more and more prominent. It is imperative that the issue be addressed with urgency in order to achieve the objectives of high-quality sustainable development within Shaanxi Province.

2.2. Data Sources

Land use/cover, DEM, and NDVI data were provided by the Resource and Environment Science and Data Center (http://www.resdc.cn/, accessed on 23 December 2023). Precipitation and evapotranspiration data were supplied by the National Earth System Science Data Center, National Science & Technology Infrastructure of China (http://www.geodata.cn/accessed on 30 December 2023). Soil attribute data were supplied by the China soil map-based harmonized world soil database. Population density was provided by LandScan (https://landscan.ornl.gov/accessed on 20 January 2024). GDP data were supplied by scientific data [43] (accessed on 23 January 2024). Night lighting data were collected from the National Tibeta Plateau Scientific Data Center (https://data.tpdc.ac.cn/accessed on 1 February 2024). Carbon consumption was supplied by Carbon Emission Accounts & Datasets (https://www.ceads.net.cn/accessed on 3 February 2024).

Water consumption data were taken from the Water Resources Bulletin. The above data are for 10 consecutive years from 2010 to 2019. Socio-economic data such as GDP per capita, disposable income of urban residents, local fiscal revenue, urbanization rate, secondary industry, and tertiary industry data are all taken from the Statistical Yearbook. These data are individual years for 2010, 2015, 2019. A detailed description is provided in Table S2. The spatial resolution and spatial coordinate system of all raster data are standardized. In order to standardize the spatial resolution of the multi-source data, 1 km × 1 km is taken as the basic unit, and all spatial data are projected using Albers projection.

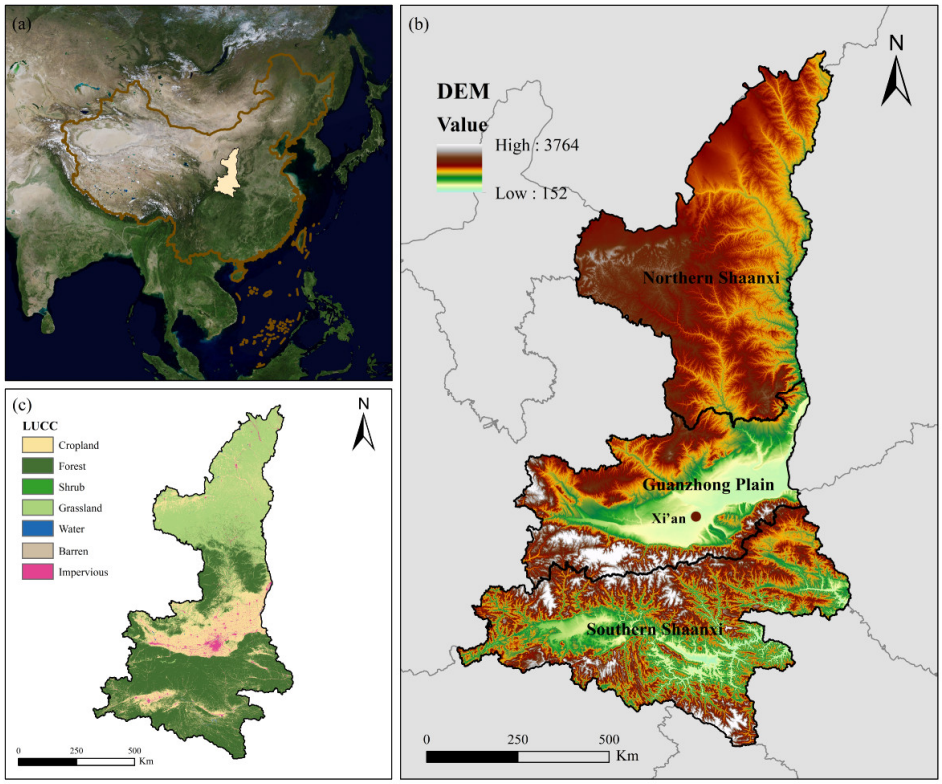


Figure 1. (**a**) Overview of Shaanxi province in China; (**b**) Elevation of Shaanxi Province; (**c**) Spatial distribution of land-use types in Shaanxi Province in 2019.

2.3. Quantification of Ecosystem Services Supply and Demand

Based on the natural background of the research area and human needs in the process of urbanization and development, we selected four key ESs, such as carbon sequestration (CS), soil conservation (SC), water yield (WY), and habitat quality (HQ). Maintaining the equilibrium of the climate and improving the biological environment depend considerably on carbon sequestration. The selection of soil conservation is based on significant soil erosion and topographical variations. The local population's survival depends heavily on water yield. Habitat quality represents the good or bad ecological environment, it is crucial to biodiversity conservation. The changes in supply and demand of the above four ESs from 2010 to 2019 were analyzed in this study. In addition, the four types of services were normalized and weighted to attain the comprehensive ecosystem services (CESs).

2.3.1. Supply of Ecosystem Services

(1) Carbon Sequestration

Carbon storage is categorized into four primary carbon pools: above-ground carbon, below-ground carbon, soil carbon, and dead organic carbon [44]. According to land use types, the carbon module of the InVEST model evaluates the carbon storage of regional ecosystems [45], as demonstrated by the calculation formula presented in Equation (1).

$$CS_S = C_{total} = C_{above} + C_{below} + C_{soil} + C_{dead} \quad (1)$$

where CS_S is supply of carbon sequestration; C_{total} denotes the overall carbon storage; C_{above} denotes above-ground carbon storage; C_{below} stands for below-ground carbon storage; C_{soil} represents soil carbon storage; C_{dead} signifies dead organic carbon storage.

(2) Soil Conservation

Research on soil conservation services plays a crucial role in assessing soil conservation levels, preventing soil degradation, and preserving soil nutrients [46]. The revised universal

soil loss equation (RUSLE) model was employed to measure soil conservation in this work. The difference between the prospective erosion rate (assuming no vegetation coverage or soil conservation practices) and the actual erosion rate (accounting for vegetation coverage, farming practices, and soil conservation measures) determines the supply of the soil conservation service. The actual soil erosion represents the need for soil conservation services. The following is the calculating formula:

$$SC_S = A_p - A_m = R \times K \times LS \times (1 - C \times P) \quad (2)$$

where A_p and A_m represent soil conservation, potential soil erosion, and actual soil erosion ($t \cdot hm^{-2} \cdot yr^{-1}$), respectively; R denotes the rainfall erosivity factor ($MJ \cdot mm \cdot hm^{-2} \cdot h^{-1} \cdot yr^{-1}$); K stands for the soil erodibility factor ($t \cdot hm^2$ h hm^{-2} $MJ^{-1}mm^{-1}$); L is the slope length factor; S refers to the slope steepness factor; C is the vegetation coverage factor; and P represents the soil and water conservation measure factor.

(3) Water Yield

The InVEST model has been extensively applied to studies of water supply services at drainage basin or regional scales [47,48]. Using information on land use, climate, and other pertinent factors, the InVEST model can calculate the water production of each grid cell. The calculations are as follows:

$$WY_S = Y_{xj} = \left(1 - \frac{AET_x}{P_x}\right) \times P_x \quad (3)$$

where WY_S represents the supply of water yield; Y_{xj} is the average annual water yield for pixel x with land cover type j; P_x is the average annual precipitation on pixel x; AET_{xj} is the average annual actual evapotranspiration for pixel x with land cover type j.

(4) Habitat quality

Habitat quality denotes the ability of an ecosystem to sustain species or populations by supplying essential resources and favorable conditions for their survival [49,50]. In this study, using relevant literature as a basis, we consider highways, provincial highways, high-speed railways, arable land, construction land, and bare land as threat sources. We then derive the habitat quality index using the habitat quality module of the InVEST model. The formula is as follows:

$$HQ_S = Q_{xj} = H_j\left(1 - \frac{{D_{xj}}^z}{{D_{xj}}^z + k^z}\right) \quad (4)$$

where HQ_S is supply of habitat quality; Q_{xj} denotes the habitat quality of grid x in landscape type j; H_j is the habitat suitability of landscape type j; D_{xj} represents the degradation degree of grid x in landscape type j; z denotes the normalization constant; and k is the half-saturation constant, the values are 2.5.

2.3.2. Demand of Ecosystem Services

(1) Carbon Sequestration

We utilized the product of per capita carbon emissions and population density to represent the demand for the carbon sequestration service in the research area. According to Carbon Emission Accounts & Datasets, the total amount of carbon emissions in Shaanxi Province from 2010 to 2019 was obtained. By dividing this total by the population, we calculated the per capita carbon emissions. We then multiplied these per capita emissions by the rasterized population density data utilizing ArcGIS 10.8.1 software to gain the carbon service demand map for the research area. The calculation formula is as follows:

$$CS_D = CS_{Dper} \times \rho_{pop} \quad (5)$$

$$CS_{Dper} = CS_{Dsum} \div \rho \quad (6)$$

where CS_D is demand of carbon sequestration; CS_{Dper} is carbon emissions per capita; ρ_{pop} is population density; CS_{Dsum} is total carbon emissions; ρ is resident population.

(2) Soil Conservation

The demand for soil conservation services is determined by the actual amount of erosion that needs to be addressed. The formula of demand for soil conservation is expressed as:

$$SC_D = R \times K \times LS \times (C \times P) \tag{7}$$

where SC_D is demand of soil conservation, the sources and explanations of the other parameters are the same as in Formula (2).

(3) Water Yield

The quota approach was utilized to estimate the need for water yield [23], which was defined as the total amount of water consumed for household, industrial, and agricultural purposes.

$$WY_D = \rho_{pop} \times x + GDP \times y + AGR \times z \tag{8}$$

where WY_D is demand of water yield; ρ_{pop} is population density; x is per capita water consumption; y is water consumption per 10,000 yuan of GDP; AGR is cropland area; z is average acre-foot water use for irrigated farmland.

(4) Habitat quality

The habitat quality need for each raster is ascertained by subtracting the habitat quality of the raster from the standard, which is the average habitat quality level in the research area. The calculation formula is as follows:

$$HQ_{Dst} = \frac{\sum_{k=1}^{M} Q_x}{S} \tag{9}$$

$$HQ_D = \begin{cases} HQ_{Dst} - Q_x, & Q_x < HQ_{Dst} \\ 0 & Q_x \geqslant HQ_{Dst} \end{cases} \tag{10}$$

where HQ_D is demand of habitat quality; HQ_{Dst} is the habitat quality demand standard; Q_x is the grid x habitat quality supply index; S is the study area (km^2).

2.4. Comprehensive Urbanization Level

Urbanization encompasses various aspects such as population growth, economic development, and expansion of construction land [31,51]. In this work, we investigate three types of urbanization: land urbanization, economic urbanization, and population urbanization. In order to create a comprehensive system of urbanization, we take four categories of data into consideration: GDP, population density, percentage of construction area, and nighttime lighting.

$$CUL = \frac{POP + GDP + NTL + CLP}{4} \tag{11}$$

where CUL represents the comprehensive urbanization level. To obtain CUL, we added the normalized values of POP, GDP, NTL, and CLP with equal weights. POP, GDP, NTL, and CLP denote the standardized value of population density, GDP, nighttime lighting, and the proportion of construction area, respectively.

2.5. Calculation of Ecosystem Services Supply–Demand Ratio

The supply and demand of ecosystem services (ESs) are linked by the ecosystem services supply–demand ratio (ESSDR), which indicates the current state of individual ES [52]. There are three possible geographical relationships between the actual ES supply

and demand: positive (surplus), negative (deficit), or zero (balancing) [53]. The calculation formula is as follows:

$$ESSDR = \frac{S - D}{\frac{(S_{max} + D_{max})}{2}} \quad (12)$$

where $ESSDR$ stands for ecological supply–demand ratio; S and D indicate the actual supply and demand of ecosystem services; S_{max} and D_{max} indicate the maximum value of the actual supply and demand of ecosystem service. An ecosystem services surplus is indicated by a number larger than 0, a deficit is shown by a value less than 0, and an equilibrium is indicated by a value of 0.

2.6. Analysis of Temporal and Spatial Changes

To identify the spatially changing patterns of the individual from 2010 onwards, a Pearson correlation analysis was employed. The calculating function is as follows:

$$r_{xy} = \frac{\sum_{i=1}^{n}(x_i - x)(y_i - y)}{\sqrt{\sum_{i=1}^{n}(x_i - x)^2}\sqrt{\sum_{i=1}^{n}(y_i - y)^2}} \quad (13)$$

where x_i, y_i are the values of two components, and x, y indicate two items' average values. The correlation coefficient between variables x and y is represented by the variable r_{xy}, which ranges from -1 to 1 ($r_{xy} > 0$, positive correlation; $r_{xy} < 0$, negative correlation).

2.7. Coupling Coordination Relationship Assessment

The degree of interplay and influence between two or more separate systems is reflected in the coupling coordination degree (CCD) [54]. The coordinated development relationship between urbanization and ESSDR can be identified using the CCD model. It can be represented using the following formulas:

$$C = 2 \times \sqrt{\frac{F_X \times G_Y}{(F_X + G_Y)^2}} \quad (14)$$

$$T = \alpha \times F_X + \beta \times G_Y \quad (15)$$

$$CCD = \sqrt{C \times T} \quad (16)$$

where C represents the coupling level, ranging from 0 to 1. A greater C value indicates a stronger interaction between CUL and ESSDR. F_X and G_Y are the CUL and ESSDR in Shaanxi, respectively. T stands for a combination of the CUL and ESSDR evaluation scores, indicating their synergistic effect. The index weights for CUL and ESSDR are shown by α and β, respectively. Since the CUL and ESSDR are regarded as equally significant in this investigation, $\alpha = \beta = 0.5$. The coupling coordination degree (CCD) for CUL and ESSDR is represented by a value between 0 and 1. Making reference to earlier research [55], this study divided CCD into four categories (Table 1).

Table 1. Classification of coupling coordination degree.

Coupling Coordination Degree	Classification
$0 \leq CCD \leq 0.3$	Severe incoordination
$0.3 < CCD \leq 0.5$	Moderate incoordination
$0.5 < CCD \leq 0.7$	Moderate coordination
$0.7 < CCD \leq 1.0$	Severe coordination

2.8. Random Forests

A decision tree-based technique called Random Forest (RF) is useful for both regression and classification [42]. A random forest is made up of several decision trees, where each tree is a composed of internal nodes that use selected features to partition the dataset into

two independent groups with comparable internal responses [56]. The importance of a feature is measured by the contribution each feature makes to the decision trees [22]. To investigate the significance of forces influencing CCD, the RF model was constructed in this study using CCD as the dependent variable and nine specifically selected indicators as the independent variables. Importance analysis based on the RF model was performed using the Random Forest package on the R Studio 3.6.0 platform.

Considering Shaanxi's natural environments, development traits, and data accessibility, we identified nine putative influencing elements that might have an impact on the CCD in our research. Among the chosen natural elements are precipitation, temperature, and topography, economic forces include per capita GDP, local fiscal revenues, and disposable income of urban residents, social forces include urbanization rate, secondary industry, and tertiary industry.

2.9. Geographically Weighted Regression (GWR) Model

The GWR model estimates local regression parameters using pertinent data from the nearby area, ultimately producing coefficients for the regression model that vary across different geographic locations [57]. In contrast to the conventional regression model, the GWR model took into account geographical location and the impact of several spatial position indices on the regression results [58]. Therefore, the GWR model can fully depict the link between independent variables and dependent variables in the distribution of various geographical areas [59]. The geographically weighted regression (GWR) model has the following formula:

$$y_i = \beta_0(u_i, v_i) + \sum \beta_k(u_i, v_i)x_{ik} + \varepsilon_i(u_i, v_i) \quad (17)$$

where y_i represents the CCD, x_{ik} represents the normalized impact factors, k represents the total amount of districts, and ε_i denotes the random error. (u_i, v_i) denotes the spatial location of sample i, $\beta_0(u_i, v_i)$ is the intercept constant of sample i, and $\beta_k(u_i, v_i)$ is the regression coefficient of the k-th spatial variable of sample i.

2.10. Quadrant Space Zoning

Based on the CCD between the regional ESSDR and CUL, the study area was divided into four regions through four quadrants in terms of two dimensions (Figure 2): the coupling level was measured by the CCD value, and the development level was measured by the CCD trend. The horizontal axis represents development level, with higher values showing stronger evolving trend of coupling coordination, and the vertical axis denotes the degree of coupling coordination, with higher values indicating stronger coordination.

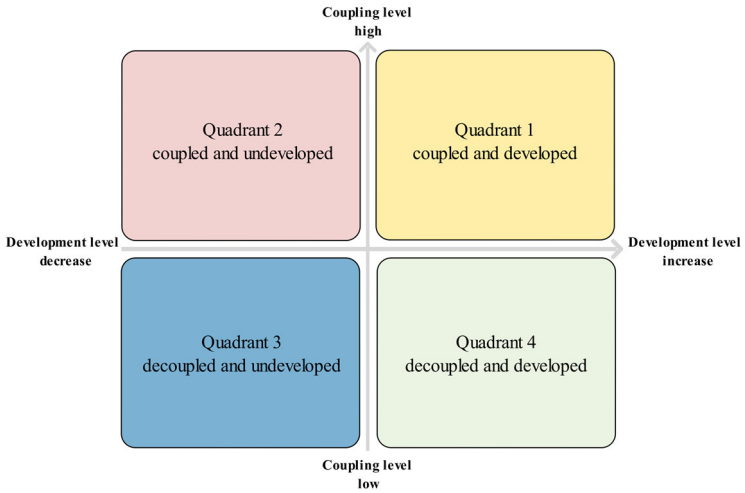


Figure 2. Quadrant space zoning.

3. Results

3.1. Changes in Supply and Demand for ES

Figure 3 illustrates the spatial distribution of changes in the supply and demand of four types of key ESs and comprehensive services from 2010 to 2019 in Shaanxi Province. During this period, the change of CS supply in Shaanxi Province was not significant, with 93.01% of the regions showing no significant change. Only 0.63% of the regions experienced a significant increase in CS supply, while 6.36% of the regions showed an obvious decreasing trend in CS, primarily concentrated in Guanzhong Plain and southern Shaanxi (Figure 3(a1)). Conversely, the demand for CS exhibited an increasing trend, indicating that economic and population growth are driving higher demand for carbon sequestration (Figure 3(a2)). The overall ESSDR of CS decreased by 98.55%, suggesting a widening gap between the supply and demand of CS (Figure 3(a3)). SC supply was decreasing in Guanzhong and northern Shaanxi, reaching 23.69% of the entire area (Figure 3(b1)). The demand of SC was growing in 19.52% of the study area, reflecting an increasing demand for soil erosion control (Figure 3(b2)). The ESSDR of SC showed no change in 54.92% of the regions and a declining trend in 41.86% of the regions (Figure 3(b3)). The supply of WY exhibited an overall decreasing trend, accounting for 93.64% of the research area, while the increased area was mainly concentrated around the Guanzhong urban agglomeration (Figure 3(c1)). The demand for WY had an increasing trend, the increasing area accounted for 78.24% of the overall area (Figure 3(c2)). The ESSDR of WY decreased by 94.61% (Figure 3(c3)), indicating an intensified conflict between the amount of water supplies available and demand. There was a decreasing trend in HQ supply and an increasing trend in HQ demand around the Guanzhong urban agglomeration (Figure 3(d1,d2)). The ESSDR of HQ decreased mainly in the Guanzhong Plain area (Figure 3(d1)). Comprehensive ecosystem services (CESs) supply and demand decreased notably by 82.43% and 69.85% (Figure 3(e1,e2)), respectively. The ESSDR of CESs decreased by 79.75% (Figure 3(e3)). However, there was a rising trend in the supply–demand ratio in the northern Shaanxi region.

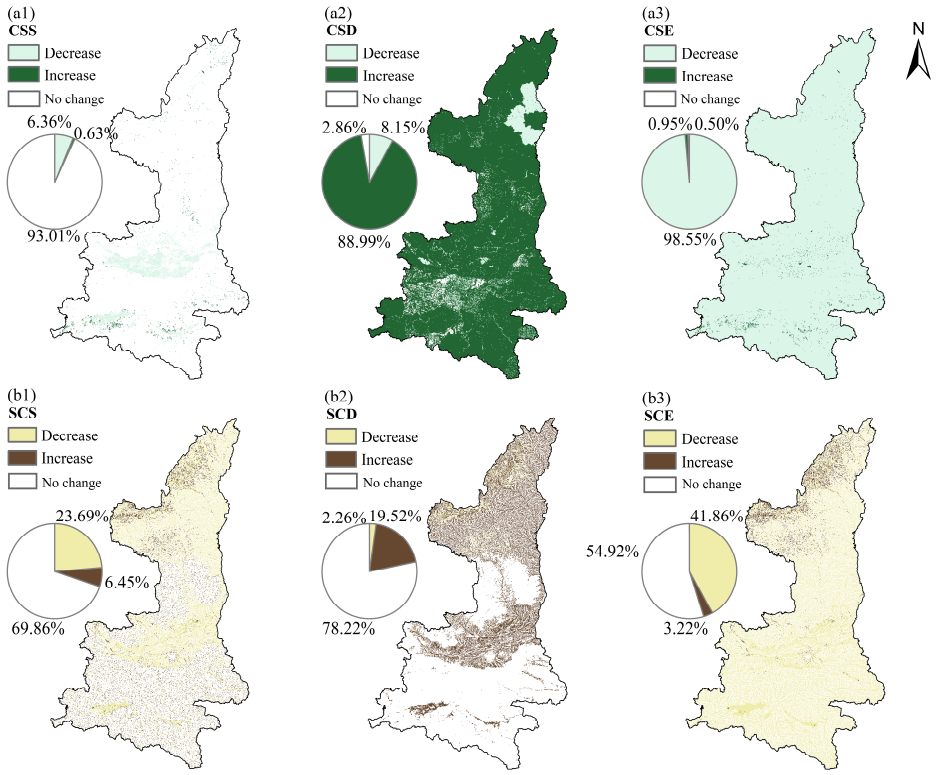


Figure 3. *Cont.*

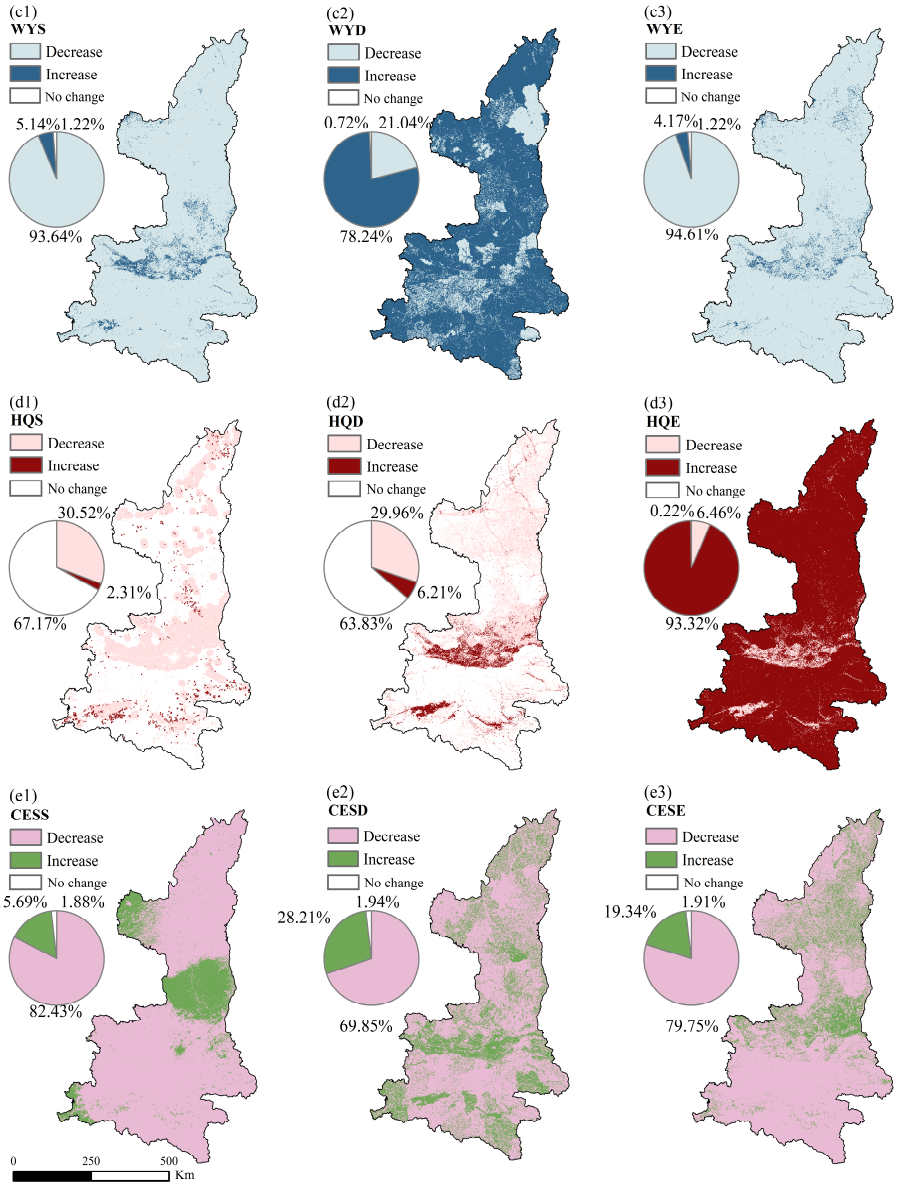


Figure 3. Trends in supply, demand, and supply–demand ratios for ecosystem services. (**a**–**e**) means CS, SC, WY, HQ and CESs; 1 means supply of ESs; 2 means demand of ESs; 3 means ESSDR of ESs.

3.2. Characteristics of Comprehensive Urbanization Levels

The spatial heterogeneity in comprehensive urbanization levels (CUL) across Shaanxi Province was notably significant (Figure 4). There was a noticeable disparity of the urbanization levels in Shaanxi Province, with the largest and most concentrated areas of urbanization located in the Xi'an Urban Agglomeration area in the Guanzhong Plain. In southern Shaanxi, influenced by the geographical barrier of the Qinling Mountains, CUL showed lower levels, and only Hanzhong and Ankang exhibited higher urbanization levels. In northern Shaanxi, the pattern of urbanization was characterized by dispersion and small-scale clusters, particularly around Yan'an and Yulin. While the urbanization level index was generally on the rise across most urban areas in Shaanxi, there were notable exceptions where it has declined, such as in Xi'an City's core district. The process of urbanization in Shaanxi Province has accelerated in recent years, leading to significant urbanization. However, this growth has not been evenly distributed, with economic and geographical forces contributing to a pronounced regional imbalance in development.

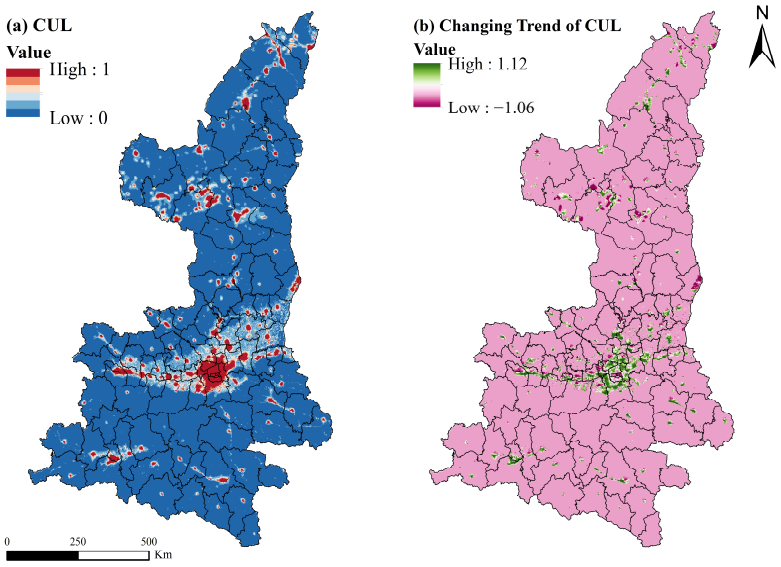


Figure 4. Level of urbanization development and trends. (**a**) Mean value of CUL from 2010 to 2019; (**b**) changing trend of CUL.

3.3. Level of Coupling Coordination and Development Trend

Figure 5 illustrates the spatial distribution and trend of the CCD in the study area over the past decade. It revealed that a majority of the counties, accounting for 52.34%, have experienced moderate incoordination between the supply–demand of ESs and the urbanization process. These areas were dispersed across Shaanxi Province. Additionally, severe incoordination was observed in 28 counties, primarily situated in the Qinling Mountains region of southern Shaanxi and the forested areas along the border between northern Shaanxi and the Guanzhong area. Meanwhile, moderate coordination was observed in 19 counties, predominantly in the Guanzhong region. Moreover, 4 counties exhibited a severe coordinated state, primarily clustered around the Xi'an metropolitan area. Despite the moderate incoordination observed in numerous regions across Shaanxi Province over the past decade, there has been a general increasing trend in CCD between supply–demand of ESs and urbanization process. Approximately 89.72% of the areas have experienced an increase in CCD, with only 10.28% of the areas demonstrated a decreasing trend.

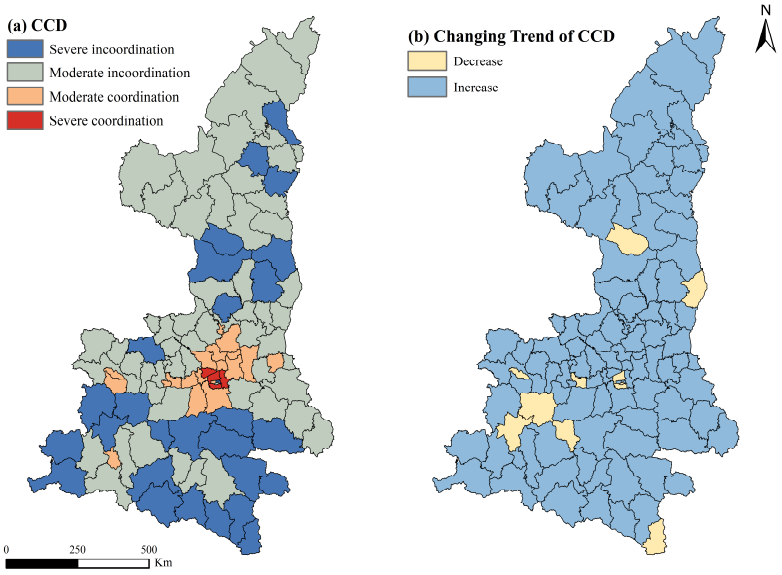


Figure 5. Level of coupling coordination degree and changing trends. (**a**) Mean value of CCD from 2010 to 2019; (**b**) changing trend of CCD.

To facilitate a comprehensive analysis of the development trend regarding the coupling coordination between the supply–demand of ESs and urbanization process in the study area, this was divided into four quadrants according to the average value and changing trend of the CCD (Figure 6). The horizontal axis indicated the level of development, with higher values denoting a greater trend of change in CCD, while the vertical axis indicated the CCD, with higher values reflecting stronger coordination. According to statistical findings, most counties (71.96%) in the research area were situated in the fourth quadrant area of the statistical map. The CCD trend in these counties was rising, although the CCD value was at a low level. Meanwhile, 17.76% of the total number of counties can be classified into the first quadrant of the statistical map. These counties maintain an increasing trend of coupling coordination with a high CCD value, which primarily clustered within the Guanzhong urban agglomeration region. Four counties, including the capital city Xi'an, were distributed in the second quadrant. These counties showed a decreasing trend of coupling coordination despite the high value of CCD. The developed regions were represented by the seven counties located in the third quadrant. These areas not only exhibited low coupling coordination but also experienced a decreasing trend in coupling coordination over time.

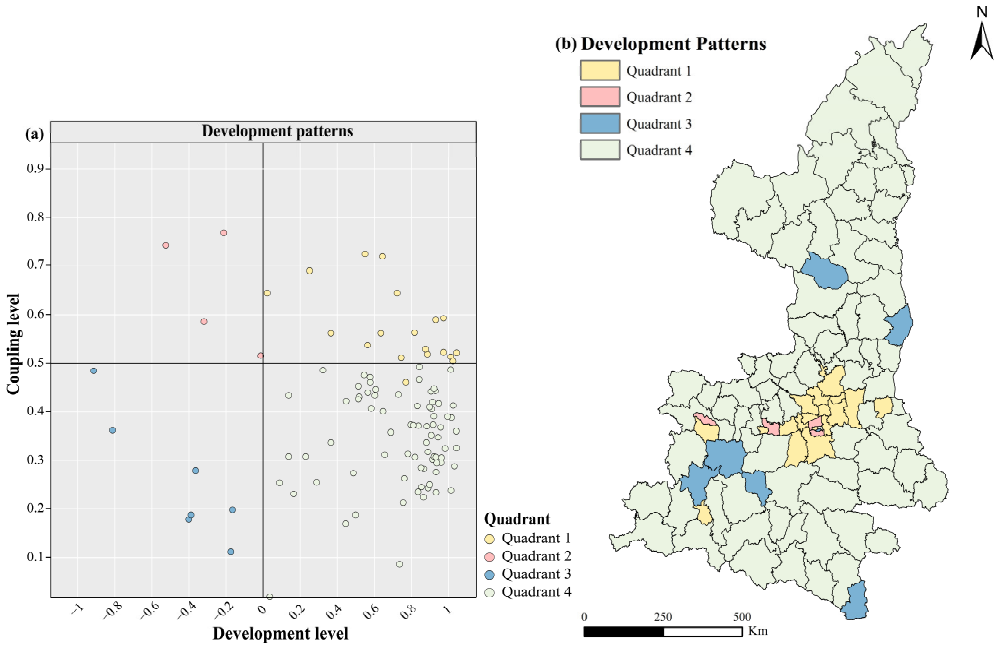


Figure 6. Development patterns of Shaanxi province from 2010 to 2019. (**a**) Quadrant distribution of development patterns; (**b**) spatial distribution of development patterns.

3.4. Driving Forces of the Coupling Coordination Relationship

To evaluate how various forces contribute to the coupling coordination between the supply–demand of ES and urbanization process, this study utilized random forests to analyze the relationship between driving forces and the counties in different development quadrants of Figure 6. The driving forces covered economic, social, and environmental forces, including per capita GDP (X1), urban residents' disposable income (X2), local fiscal revenue (X3), urbanization rate (X4), secondary industry (X5), tertiary industry (X6), precipitation (X7), temperature (X8), and topography (X9). The results in Table 2 and Figure 7 show that, for counties situated in the first quadrant, characterized by a high CCD and a positive trend in development, the tertiary industry (X6) exhibited a notable increase in importance, rising from 6.02% in 2010 to 22.56% in 2019, becoming the most influential force. Conversely, the disposable income of urban residents (X2) experienced a significant decrease from 25.69% in 2010 to 6.32% in 2019. This shift indicated a growing prominence of social forces in influencing the coupling coordination process. In the second quadrant, in

which counties maintained a high level of CCD but experienced a decreasing trend, GDP per capita (X1) had the largest proportion of importance. However, the disposable income of urban residents (X2) occupied an increased proportion of importance over time with a significant change of 13.83%. For counties in the third quadrant, GDP per capita (X1) had steadily increased. Meanwhile, topographical forces (X9) demonstrated the greatest importance, experiencing a significant increase of 4.62%. Both environmental and economic forces contributed significantly to this quadrant of counties. In the fourth quadrant, in which counties had a low but a positive change trend of CCD, the importance of disposable income of urban residents (X2) and local revenues (X3) increased. Conversely, the impact of secondary industry (X5) showed a sharp decrease.

Table 2. Importance of forces to variations in CCD in 2010, 2015, and 2019.

	Year	X1	X2	X3	X4	X5	X6	X7	X8	X9
Quadrant 1	2010	13.84	25.69	9.08	8.02	5.25	6.02	4.92	16.23	10.95
	2015	18.01	20.08	9.89	7.03	6.98	5.29	5.73	9.48	17.5
	2019	8.08	6.32	19.68	14.33	4.28	22.56	4.37	14.78	5.61
Quadrant 2	2010	18.97	1.83	9.64	13.03	6.99	10.44	11.86	16.51	10.73
	2015	14.98	14.4	9.33	9.96	7.79	10.85	6.24	16.23	10.21
	2019	18.27	15.66	9.57	10.17	7.08	8.97	9.12	12.03	9.14
Quadrant 3	2010	11.65	16.58	9.09	9.26	5.59	10	4.58	16.69	17.04
	2015	13.37	10.67	10.49	15.87	8.49	7.22	4.86	9.59	19.43
	2019	14.05	16.06	8.82	12.5	4.17	9.19	2.52	11.03	21.66
Quadrant 4	2010	2.17	12.49	5.53	3.75	32.37	15.89	10.84	9.76	7.21
	2015	3.23	6.83	3.11	9.75	19.07	16.02	21.93	8.52	11.56
	2019	4.5	16.8	17.14	13.06	2.51	16.51	2.34	20.74	6.41

Note: X1–per capita GDP, X2–urban residents' disposable income, X3–local fiscal revenue, X4–urbanization rate, X5–secondary industry, X6–tertiary industry, X7–precipitation, X8–temperature, X9–topography.

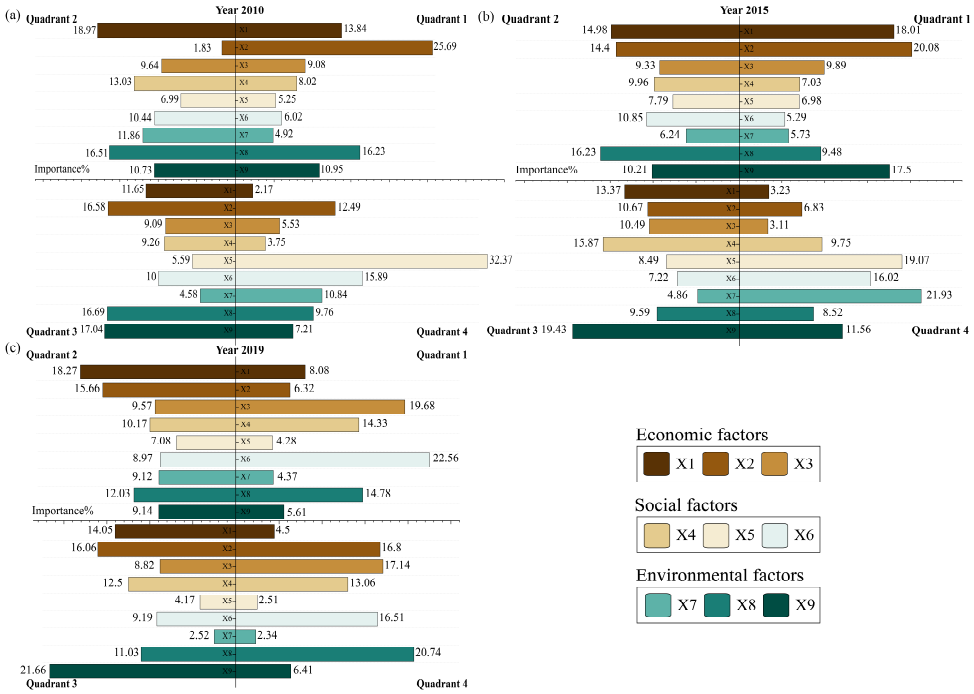


Figure 7. (**a**) Importance of forces to variations in CCD in 2010; (**b**) Importance of forces to variations in CCD in 2015; (**c**) Importance of forces to variations in CCD in 2019. X1–per capita GDP, X2–urban residents' disposable income, X3–local fiscal revenue, X4–urbanization rate, X5–secondary industry, X6–tertiary industry, X7–precipitation, X8–temperature, X9–topography.

In order to further reveal the regional variations in driving forces of CCD, this study employed geographically weighted regression to explore the spatial distribution of the impact forces as well as the degree of importance (Figure 8). The results showed that per capita GDP (X1), local fiscal revenue (X3), tertiary industry (X6), temperature (X8), and topography (X9) exhibited a transition from negative to positive correlation. Except for local fiscal revenue (X3), the positive influence of these forces decreased from north to south. In terms of spatial distribution, per capita GDP (X1), local fiscal revenue (X3), temperature (X8), and topography (X9) predominantly shifted from negative correlation in southern Shaanxi to positive correlation in northern Shaanxi. Conversely, tertiary industry (X6) transitioned from significant negative correlation in northern Shaanxi to positive correlation. Disposable income of urban residents (X2), secondary industry (X5), and precipitation (X7) transitioned from positive correlation to negative correlation, albeit with distinct regional variations. Among them, the disposable income of urban residents (X2) transitioned from positive to negative correlation in southern Shaanxi, secondary industry (X5) exhibited a negative correlation across the entire region, and precipitation (X7) shifted to negative correlation primarily in northern Shaanxi. Urbanization rate (X4) consistently displayed a positive correlation, with its influence intensifying from north to south, and the impact reached the highest in 2019.

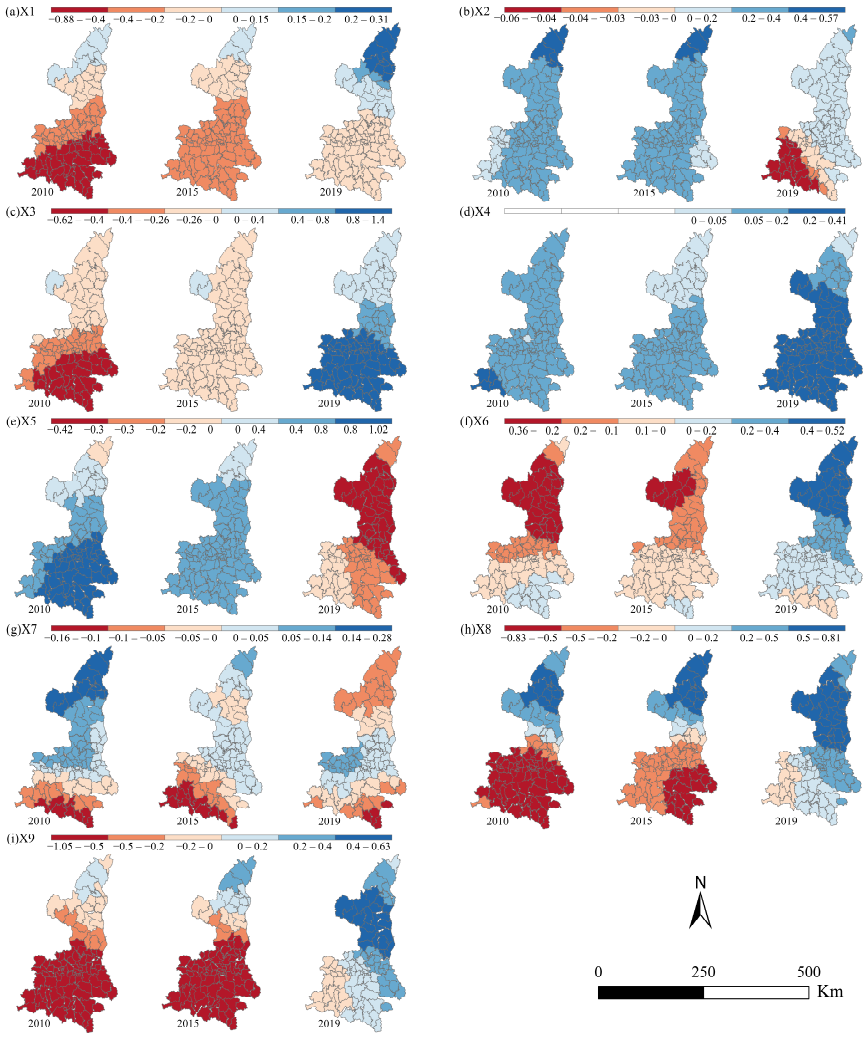


Figure 8. Regression coefficient spatial patterns in the estimation of CCD in 2010, 2015, and 2019. (**a**) X1–per capita GDP, (**b**) X2–an residents' disposable income, (**c**) X3–local fiscal revenue, (**d**) X4–urbanization rate, (**e**) X5–secondary industry, (**f**) X6–tertiary industry, (**g**) X7–precipitation, (**h**) X8–temperature, (**i**) X9–topography.

4. Discussion

4.1. Changes in ESSDR

Quantifying the mismatch between supply and demand among ES can provide valuable insights for guiding ecological management and landscape planning [60,61]. This research finds that there is an excess of demand in more urbanized areas, while there is a general oversupply in ecologically healthy areas, and this varies with the characteristics of the urbanization process in the various regions of northern Shaanxi, Guanzhong, and southern Shaanxi. This pattern is also reflected in other investigations [17,62].

Except for water yield services, which are more abundant in Guanzhong (Figure 9(c1)), the supply and demand of other services follow a similar distribution in the region. Urbanization driving shifts in land use types is identified as a main driver affecting ESs. Among different land use types, forested and grassland areas exhibit the highest capacities for carbon sequestration, in stark contrast to construction lands, which show the lowest [63]. However, compared to grassland and forested regions, construction areas have lower levels of water infiltration, evapotranspiration, and retention [64]. There is a deficit of supply and demand for all services (Figure 9), and this gap is widening (Figure 3). ES consumption is closely related to socio-economics, the region's dense economic activities and rising population density aggravate services consumption, and rapid economic expansion has led to increased demand for services [65]. In the face of this situation, it is essential for the government to explore various strategies to augment ES supply, such as the promotion of green transportation, the expansion of public green space, which can effectively alleviate the phenomenon of insufficient supply of habitat quality and carbon sequestration [66]. However, unless the ES demand decreases, the effect of solving the mismatch between supply and demand by locally increasing the supply of ES is limited. Therefore, it is crucial to implement measures to define the boundary of urban expansion, control the growth of the population, manage industrial carbon emissions effectively, and prevent encroachment on natural lands [67].

In northern Shaanxi, the soil conservation capacity is notably limited due to its fragile ecological environment and inadequate vegetation cover, which inefficiently intercepts precipitation. This challenge is compounded by the region's arid and semi-arid climate [68]. Nevertheless, ecological projects in the area have led to improvements in soil conservation and a reduction in soil erosion, resulting in the supply–demand ratio for soil conservation to rise in some regions (Figure 3(b3)) [69]. The gap between supply and demand for water production and carbon sequestration services is also more pronounced in individual areas where urbanization is more pronounced (Figure 9(a3,c3)). This deficit is distributed in a scattered pattern that aligns with the extent of urbanization (Figure 4). Notably, as the ecological projects are being implemented in northern Shaanxi, the effect of habitat improvement has been significant. These initiatives have progressively narrowed the gap between supply and demand for different services, thereby alleviating existing contradictions (Figure 3). In the future, it is essential to continue ecological restoration efforts, building on the foundation of Grain to Green Projects, to enhance the ecological functions of diverse services.

Benefiting from the vast forest area, high vegetation cover and rich biodiversity, the overall ecological environment in southern Shaanxi is relatively healthy, with a surplus of all types of services (Figure 9). With the development of urbanization, the coupling relationship between urbanization and supply–demand of ES has improved (Figure 5). However, in more urbanized areas like Hanzhong and Ankang, there remains a deficit state, where the discrepancy between supply and demand for services is widening, and the contradiction between them is becoming more obvious (Figure 3). Given the superior ecological environment of southern Shaanxi, it is advisable to strategically leverage these ecological advantages. Implementing production methods tailored to local conditions can help maintain and even enhance ES capacities, thereby addressing the growing supply–demand challenges in urbanized areas.

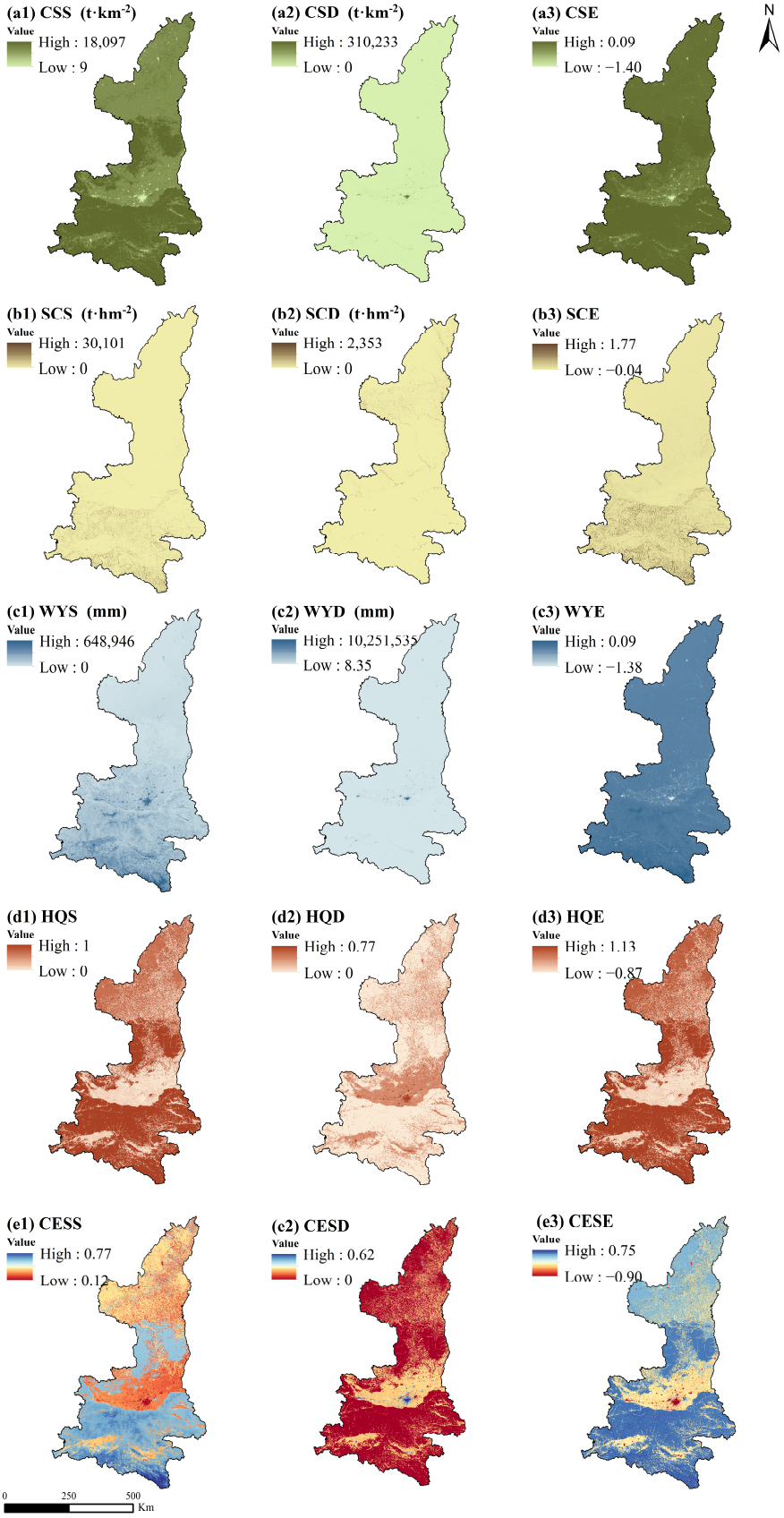


Figure 9. Distribution of ecosystem services supply, demand, and supply–demand ratios. (**a**–**e**) means CS, SC, WY, HQ and CESs; 1 means supply of ES; 2 means demand of ES; 3 means ESSDR of ESs.

4.2. Driving Forces of CCD

The interplay between the supply–demand ratio of ES and urbanization process exhibits pronounced regional differences, necessitating that regional development strategies be informed by the integration and coordination of ES, with urbanization levels. This study analyzed the coupling coordination relationship between urbanization and supply–demand of ESs across Shaanxi Province and found an overall upward trend in CCD. However, this general trend is distinguished by different spatio-temporal characteristics in different counties. According to the spatio-temporal distribution of CCD shown in Figure 6, counties in the first quadrant exhibited a high and increasing CCD over time. Initially, the main driver of this relationship in these areas was urban residents' disposable income. As the CCD increased, the driving forces evolved, with tertiary industry and local fiscal revenue becoming predominant (Figure 7 and Table 2). The rise in CCD is positively impacted by these two variables, as shown in Figure 8c,f. The tertiary industry's quick growth significantly boosts the regional socio-economic status. Established advanced industrial clusters, like high-tech parks and development zones, not only improve resource allocation efficiency but also enhance carbon efficiency through industrial concentration, facilitating harmonious development [70,71]. In later stages, this coordinated development necessitates collective efforts from both government and society, including heightened investments in ecological conservation and public awareness on environmental management, aiming to improve the region's ecological quality [72].

The results in Figure 6 demonstrated that over the past decade, the counties within the fourth quadrant presented low levels but a continuous upward trend of CCD. The primary influence forces in these regions were secondary industry, tertiary industry, financial income, and temperature (Figure 7 and Table 2). The majority of counties in Shaanxi Province exhibited relatively low urbanization levels at the start of the study session (Figure 4). The implementation of large-scale industrial construction has been demonstrated to effectively promote the acceleration of urbanization [73]. Consequently, secondary industry has been observed to exert a discernible positive influence on the increase in CCD (Figure 8e). However, with the expansion of industrial scale, the conflict between the supply and demand of regional ES has become increasingly pronounced [74]. As the study progressed into later stages, the impact of secondary industry on CCD shifted to a negative correlation, while forces such as tertiary industry and financial income began to dominate and positively influence the growth of CCD. Similar to the counties in the first quadrant, harmonious social and ecological development in the region will require the increase in financial investment, implement ecological compensation policies, and rationally plan urban production [75]. The influence of natural forces on CCD is notably complex, particularly the impact on ESs. Shaanxi Province is in the dry and semi-arid area of the Loess Plateau. An increase in temperature alone will intensify drought and negatively affect ecosystem development. However, recent studies indicated a shift in the climate of the study area from a gradual warming to a warmer and more humid pattern. This climatic change had effectively extended the growing season for regional vegetation, promoting the development of vegetation ecosystems (Figure 8h) [76,77].

Counties in the third quadrant exhibited the most challenging state of coupling coordination, characterized by both low levels and a decreasing trend in CCD. These counties are primarily situated in the Taibai Mountain area within the Qinling Mountains, where topographical forces significantly constrain their development, typically exerting a negative impact on CCD (Figure 8i). The rugged terrain of the Qinling Mountains limits the potential for urban expansion in the surrounding counties. Nonetheless, considering how vital it is to preserve the environment and ecosystem in the Qinling region, it may be suitable to allow decoupled development between urbanization and ESs in these areas. Additionally, the counties in the second quadrant also showed a declining trend of CCD. They are the least numerous and have a high CCD level, and they are situated in the central urban area of the Xi'an-Xianyang urban agglomeration. This central area is characterized by highly urbanized and economically developed, with economic forces (X1X2) becoming the

principal drivers influencing CCD (Figure 7 and Table 2). However, economic development in this region tends to place a greater burden on the supply and demand of services, and the influences are predominantly negative.

4.3. Limitations and Prospect

There are still several issues that need to be resolved, even if this study can offer insightful information about ecosystem sustainability by quantifying the coupling coordination between ES supply–demand and urbanization. The study focus on just four key ES categories may not fully capture the ecological conditions of Shaanxi Province, a region celebrated for its unique natural landscapes and rich cultural heritage. Incorporating cultural services and additional indicators like air quality and food production could provide a more holistic view of the ecosystem. Urbanization is not only about population agglomeration, economic growth, and expansion of construction land, but also about the enhancement of population quality and the development of urban green space [78]. Therefore, in future we will obtain more data on ES types and sociocultural urbanization to develop a more systematic understanding of coupling coordination between ecosystem and urbanization. Furthermore, it is feasible to contemplate the effects of urbanization on an individual service and ascertain the extent of these effects, thereby facilitating a more all-encompassing comprehension of the impact of urbanization on services.

5. Conclusions

This research assessed the spatial and temporal variations in the supply and demand of four key ESs as well as urbanization from 2010 to 2019, explored the coupling coordination relationship between them, and explored the driving forces that affect CCD. The results demonstrated that (1) the supply of four ESs experienced a decline trend, demand increased significantly within the Guanzhong Urban Agglomeration. Moreover, except for habitat quality, the supply–demand ratios of other services displayed a decreasing trend, indicating a spatial imbalance. Significant disparities in urbanization levels were observed in Shaanxi Province; (2) Significant disparities in urbanization levels were observed in Shaanxi Province, the urbanization level of most areas was on an upward trend, with the Guanzhong Plain Xi'an urban agglomeration emerging as the core area of urbanization; (3) The majority of areas exhibited a lack of coordination between ESs and the urbanization process. However, there was an overarching upward trend in CCD; (4) According to the results of the partition of CCD, the first and fourth quadrants contained quite a few of the counties. Counties in these quadrants have demonstrated an increasing trend in CCD. Influence forces such as tertiary industry and fiscal revenue gradually take the dominant position, positively effecting the growth of CCD. The counties in the second quadrant have the least number, showed a decreasing trend of CCD, with economic forces becoming the principal drivers negatively influencing CCD. The counties in the third quadrant exhibited a low and decreasing CCD, primarily constrained by mountain range. The topographic forces in these areas negatively impact CCD. In light of these findings, urban ecological management strategies should prioritize balancing the supply and demand of ESs, optimizing economic layouts to accommodate regional disparities, and fostering coordination between social development and the ecological environment. Targeted policies are necessary to harmonize the sustainable development of the region, accounting for the intricate interactions between urbanization and ESs.

Supplementary Materials: The following supporting information can be downloaded at: https://www.mdpi.com/article/10.3390/rs16132383/s1, Figure S1: Administrative maps of northern Shaanxi, Guanzhong, and southern Shaanxi.; Table S1: County characteristics data (2019); Table S2: Driving forces data.

Author Contributions: Conceptualization, J.L. and H.W.; methodology, J.L. and H.W.; software, J.L. and L.H.; formal analysis, B.T. and L.H.; visualization, J.L. and B.T.; supervision, L.Z. and L.J.; funding acquisition, H.W.; writing—original draft preparation, J.L.; writing—review and editing, H.W. All authors have read and agreed to the published version of the manuscript.

Funding: This research was funded by [Natural Science Basic Research Plan in Shaanxi Province of China] grant number [2023-JC-YB-229], [National Natural Science Foundation of China] grant number [No. 42371103].

Data Availability Statement: The original contributions of this study are included in this article. Further inquiries can be directed to the corresponding authors.

Conflicts of Interest: The authors declare no conflicts of interest.

References

1. Costanza, R.; d'Arge, R.; de Groot, R.; Farber, S.; Grasso, M.; Hannon, B.; Limburg, K.; Naeem, S.; O'Neill, R.V.; Paruelo, J.; et al. The value of the world's ecosystem services and natural capital. *Nature* **1997**, *387*, 253–260. [CrossRef]
2. Gao-Di, X.; Yu, X.; Chun-Xia, L. Institute of Geographic Sciences and Natural Resources Research, Chinese Academy of Sciences, Beijing 100101, China study on ecosystem services: Progress, limitation and basic paradigm. *Chin. J. Plant Ecol.* **2006**, *30*, 191–199. [CrossRef]
3. Villamagna, A.M.; Angermeier, P.L.; Bennett, E.M. Capacity, Pressure, Demand, and Flow: A Conceptual Framework for Analyzing Ecosystem Service Provision and Delivery. *Ecol. Complex.* **2013**, *15*, 114–121. [CrossRef]
4. Wei, H.; Fan, W.; Wang, X.; Lu, N.; Dong, X.; Zhao, Y.; Ya, X.; Zhao, Y. Integrating Supply and Social Demand in Ecosystem Services Assessment: A Review. *Ecosyst. Serv.* **2017**, *25*, 15–27. [CrossRef]
5. Maes, J.; Crossman, N.D.; Burkhard, B. Mapping Ecosystem Services. In *Routledge Handbook of Ecosystem Services*; Routledge: London, UK, 2016.
6. Schirpke, U.; Candiago, S.; Egarter Vigl, L.; Jäger, H.; Labadini, A.; Marsoner, T.; Meisch, C.; Tasser, E.; Tappeiner, U. Integrating Supply, Flow and Demand to Enhance the Understanding of Interactions among Multiple Ecosystem Services. *Sci. Total Environ.* **2019**, *651*, 928–941. [CrossRef]
7. Li, J.; Jiang, H.; Bai, Y.; Alatalo, J.M.; Li, X.; Jiang, H.; Liu, G.; Xu, J. Indicators for Spatial–Temporal Comparisons of Ecosystem Service Status between Regions: A Case Study of the Taihu River Basin, China. *Ecol. Indic.* **2016**, *60*, 1008–1016. [CrossRef]
8. Sun, X.; Tang, H.; Yang, P.; Hu, G.; Liu, Z.; Wu, J. Spatiotemporal Patterns and Drivers of Ecosystem Service Supply and Demand across the Conterminous United States: A Multiscale Analysis. *Sci. Total Environ.* **2020**, *703*, 135005. [CrossRef] [PubMed]
9. Chen, D.; Li, J.; Yang, X.; Zhou, Z.; Pan, Y.; Li, M. Quantifying Water Provision Service Supply, Demand and Spatial Flow for Land Use Optimization: A Case Study in the YanHe Watershed. *Ecosyst. Serv.* **2020**, *43*, 101117. [CrossRef]
10. Wei, H.; Liu, H.; Xu, Z.; Ren, J.; Lu, N.; Fan, W.; Zhang, P.; Dong, X. Linking Ecosystem Services Supply, Social Demand and Human Well-Being in a Typical Mountain–Oasis–Desert Area, Xinjiang, China. *Ecosyst. Serv.* **2018**, *31*, 44–57. [CrossRef]
11. Wolff, S.; Schulp, C.J.E.; Kastner, T.; Verburg, P.H. Quantifying Spatial Variation in Ecosystem Services Demand: A Global Mapping Approach. *Ecol. Econ.* **2017**, *136*, 14–29. [CrossRef]
12. Ghasemi, M.; González-García, A.; Charrahy, Z.; Serrao-Neumann, S. Utilizing Supply-Demand Bundles in Nature-Based Recreation Offers Insights into Specific Strategies for Sustainable Tourism Management. *Sci. Total Environ.* **2024**, *922*, 171185. [CrossRef] [PubMed]
13. Liu, Q.; Liu, H.; Xu, G.; Lu, B.; Wang, X.; Li, J. Spatial Gradients of Supply and Demand of Ecosystem Services within Cities. *Ecol. Indic.* **2023**, *157*, 111263. [CrossRef]
14. Leemans, R.; De Groot, R.S. *Ecosystems and Human Well-Being: Synthesis*; Millennium Ecosystem Assessment (Program), Ed.; Island Press: Washington, DC, USA, 2005; ISBN 978-1-59726-040-4.
15. Arunrat, N.; Sereenonchai, S.; Wang, C. Carbon Footprint and Predicting the Impact of Climate Change on Carbon Sequestration Ecosystem Services of Organic Rice Farming and Conventional Rice Farming: A Case Study in Phichit Province, Thailand. *J. Environ. Manag.* **2021**, *289*, 112458. [CrossRef] [PubMed]
16. Bai, Y.; Wong, C.P.; Jiang, B.; Hughes, A.C.; Wang, M.; Wang, Q. Developing China's Ecological Redline Policy Using Ecosystem Services Assessments for Land Use Planning. *Nat. Commun.* **2018**, *9*, 3034. [CrossRef] [PubMed]
17. Baró, F.; Palomo, I.; Zulian, G.; Vizcaino, P.; Haase, D.; Gómez-Baggethun, E. Mapping Ecosystem Service Capacity, Flow and Demand for Landscape and Urban Planning: A Case Study in the Barcelona Metropolitan Region. *Land Use Policy* **2016**, *57*, 405–417. [CrossRef]
18. Huang, L.; Wang, J.; Fang, Y.; Zhai, T.; Cheng, H. An Integrated Approach towards Spatial Identification of Restored and Conserved Priority Areas of Ecological Network for Implementation Planning in Metropolitan Region. *Sustain. Cities Soc.* **2021**, *69*, 102865. [CrossRef]
19. Chen, G.; Li, X.; Liu, X.; Chen, Y.; Liang, X.; Leng, J.; Xu, X.; Liao, W.; Qiu, Y.; Wu, Q.; et al. Global Projections of Future Urban Land Expansion under Shared Socioeconomic Pathways. *Nat. Commun.* **2020**, *11*, 537. [CrossRef] [PubMed]

20. Liu, L.; Wu, J. Ecosystem Services-Human Wellbeing Relationships Vary with Spatial Scales and Indicators: The Case of China. *Resour. Conserv. Recycl.* **2021**, *172*, 105662. [CrossRef]
21. Pan, Z.; Wang, J. Spatially Heterogeneity Response of Ecosystem Services Supply and Demand to Urbanization in China. *Ecol. Eng.* **2021**, *169*, 106303. [CrossRef]
22. Zhang, Z.; Peng, J.; Xu, Z.; Wang, X.; Meersmans, J. Ecosystem Services Supply and Demand Response to Urbanization: A Case Study of the Pearl River Delta, China. *Ecosyst. Serv.* **2021**, *49*, 101274. [CrossRef]
23. González-García, A.; Palomo, I.; González, J.A.; López, C.A.; Montes, C. Quantifying Spatial Supply-Demand Mismatches in Ecosystem Services Provides Insights for Land-Use Planning. *Land Use Policy* **2020**, *94*, 104493. [CrossRef]
24. Shi, Y.; Shi, D.; Zhou, L.; Fang, R. Identification of Ecosystem Services Supply and Demand Areas and Simulation of Ecosystem Service Flows in Shanghai. *Ecol. Indic.* **2020**, *115*, 106418. [CrossRef]
25. Cumming, G.S.; Buerkert, A.; Hoffmann, E.M.; Schlecht, E.; Von Cramon-Taubadel, S.; Tscharntke, T. Implications of Agricultural Transitions and Urbanization for Ecosystem Services. *Nature* **2014**, *515*, 50–57. [CrossRef] [PubMed]
26. Peng, J.; Wang, X.; Liu, Y.; Zhao, Y.; Xu, Z.; Zhao, M.; Qiu, S.; Wu, J. Urbanization Impact on the Supply-Demand Budget of Ecosystem Services: Decoupling Analysis. *Ecosyst. Serv.* **2020**, *44*, 101139. [CrossRef]
27. Yang, Z.; Hu, J.; Wang, Z.; Chen, S. A New Model Based on Coupling Coordination Analysis Incorporates the Development Rate for Urbanization and Ecosystem Services Assessment: A Case of the Yangtze River Delta. *Ecol. Indic.* **2024**, *159*, 111596. [CrossRef]
28. Kadhim, N.; Ismael, N.T.; Kadhim, N.M. Urban Landscape Fragmentation as an Indicator of Urban Expansion Using Sentinel-2 Imageries. *Civ. Eng. J.* **2022**, *8*, 1799–1814. [CrossRef]
29. Kumar, D.; Soni, A.; Kumar, M. Retrieval of Land Surface Temperature from Landsat-8 Thermal Infrared Sensor Data. *J. Hum. Earth Future* **2022**, *3*, 159–168. [CrossRef]
30. Wei, H.; Xue, D.; Huang, J.; Liu, M.; Li, L. Identification of Coupling Relationship between Ecosystem Services and Urbanization for Supporting Ecological Management: A Case Study on Areas along the Yellow River of Henan Province. *Remote Sens.* **2022**, *14*, 2277. [CrossRef]
31. Ding, T.; Chen, J.; Fang, Z.; Chen, J. Assessment of Coordinative Relationship between Comprehensive Ecosystem Service and Urbanization: A Case Study of Yangtze River Delta Urban Agglomerations, China. *Ecol. Indic.* **2021**, *133*, 108454. [CrossRef]
32. Zhao, H.; Li, C.; Gao, M. Investigation of the Relationship between Supply and Demand of Ecosystem Services and the Influencing Factors in Resource-Based Cities in China. *Sustainability* **2023**, *15*, 7397. [CrossRef]
33. Song, Y.; Wang, J.; Ge, Y.; Xu, C. An Optimal Parameters-Based Geographical Detector Model Enhances Geographic Characteristics of Explanatory Variables for Spatial Heterogeneity Analysis: Cases with Different Types of Spatial Data. *GIScience Remote Sens.* **2020**, *57*, 593–610. [CrossRef]
34. Hou, W.; Hu, T.; Yang, L.; Liu, X.; Zheng, X.; Pan, H.; Zhang, X.; Xiao, S.; Deng, S. Matching Ecosystem Services Supply and Demand in China's Urban Agglomerations for Multiple-Scale Management. *J. Clean. Prod.* **2023**, *420*, 138351. [CrossRef]
35. Negev, M.; Sagie, H.; Orenstein, D.E.; Zemah Shamir, S.; Hassan, Y.; Amasha, H.; Raviv, O.; Fares, N.; Lotan, A.; Peled, Y.; et al. Using the Ecosystem Services Framework for Defining Diverse Human-Nature Relationships in a Multi-Ethnic Biosphere Reserve. *Ecosyst. Serv.* **2019**, *39*, 100989. [CrossRef]
36. Khosravi Mashizi, A.; Sharafatmandrad, M. Investigating Tradeoffs between Supply, Use and Demand of Ecosystem Services and Their Effective Drivers for Sustainable Environmental Management. *J. Environ. Manag.* **2021**, *289*, 112534. [CrossRef] [PubMed]
37. Li, J.; Xie, B.; Dong, H.; Zhou, K.; Zhang, X. The Impact of Urbanization on Ecosystem Services: Both Time and Space Are Important to Identify Driving Forces. *J. Environ. Manag.* **2023**, *347*, 119161. [CrossRef] [PubMed]
38. Zhu, C.; Zhang, X.; Zhou, M.; He, S.; Gan, M.; Yang, L.; Wang, K. Impacts of Urbanization and Landscape Pattern on Habitat Quality Using OLS and GWR Models in Hangzhou, China. *Ecol. Indic.* **2020**, *117*, 106654. [CrossRef]
39. Hu, J.; Zhang, J.; Li, Y. Exploring the Spatial and Temporal Driving Mechanisms of Landscape Patterns on Habitat Quality in a City Undergoing Rapid Urbanization Based on GTWR and MGWR: The Case of Nanjing, China. *Ecol. Indic.* **2022**, *143*, 109333. [CrossRef]
40. Ma, S.; Wang, L.; Wang, H.; Zhang, X.; Jiang, J. Spatial Heterogeneity of Ecosystem Services in Response to Landscape Patterns under the Grain for Green Program: A Case-study in Kaihua County, China. *Land Degrad. Dev.* **2022**, *33*, 1901–1916. [CrossRef]
41. Wang, L.-J.; Gong, J.-W.; Ma, S.; Wu, S.; Zhang, X.; Jiang, J. Ecosystem Service Supply–Demand and Socioecological Drivers at Different Spatial Scales in Zhejiang Province, China. *Ecol. Indic.* **2022**, *140*, 109058. [CrossRef]
42. Wu, J.; Guo, X.; Zhu, Q.; Guo, J.; Han, Y.; Zhong, L.; Liu, S. Threshold Effects and Supply-Demand Ratios Should Be Considered in the Mechanisms Driving Ecosystem Services. *Ecol. Indic.* **2022**, *142*, 109281. [CrossRef]
43. Chen, J.; Gao, M.; Cheng, S.; Cheng, G.S. Global 1 km × 1 km gridded revised real gross domestic product and electricity consumption during 1992–2019 based on calibrated nighttime light data. *Sci Data* **2022**, *9*, 202. [CrossRef] [PubMed]
44. Bacani, V.M.; Machado Da Silva, B.H.; Ayumi De Souza Amede Sato, A.; Souza Sampaio, B.D.; Rodrigues Da Cunha, E.; Pereira Vick, E.; Ribeiro De Oliveira, V.F.; Decco, H.F. Carbon Storage and Sequestration in a Eucalyptus Productive Zone in the Brazilian Cerrado, Using the Ca-Markov/Random Forest and InVEST Models. *J. Clean. Prod.* **2024**, *444*, 141291. [CrossRef]
45. Wang, Y.; Li, M.; Jin, G. Exploring the Optimization of Spatial Patterns for Carbon Sequestration Services Based on Multi-Scenario Land Use/Cover Changes in the Changchun-Jilin-Tumen Region, China. *J. Clean. Prod.* **2024**, *438*, 140788. [CrossRef]
46. Phinzi, K.; Ngetar, N.S. The Assessment of Water-Borne Erosion at Catchment Level Using GIS-Based RUSLE and Remote Sensing: A Review. *Int. Soil Water Conserv. Res.* **2019**, *7*, 27–46. [CrossRef]

47. Liu, M.; Dong, X.; Zhang, Y.; Wang, X.; Wei, H.; Zhang, P.; Zhang, Y. Spatiotemporal Changes in Future Water Yield and the Driving Factors under the Carbon Neutrality Target in Qinghai. *Ecol. Indic.* **2024**, *158*, 111310. [CrossRef]
48. Qiu, H.; Zhang, J.; Han, H.; Cheng, X.; Kang, F. Study on the Impact of Vegetation Change on Ecosystem Services in the Loess Plateau, China. *Ecol. Indic.* **2023**, *154*, 110812. [CrossRef]
49. Hillard, E.M.; Nielsen, C.K.; Groninger, J.W. Swamp Rabbits as Indicators of Wildlife Habitat Quality in Bottomland Hardwood Forest Ecosystems. *Ecol. Indic.* **2017**, *79*, 47–53. [CrossRef]
50. Zhang, X.; Wan, W.; Fan, H.; Dong, X.; Lv, T. Temporal and Spatial Responses of Landscape Patterns to Habitat Quality Changes in the Poyang Lake Region, China. *J. Nat. Conserv.* **2024**, *77*, 126546. [CrossRef]
51. Tian, Y.; Zhou, D.; Jiang, G. Conflict or Coordination? Multiscale Assessment of the Spatio-Temporal Coupling Relationship between Urbanization and Ecosystem Services: The Case of the Jingjinji Region, China. *Ecol. Indic.* **2020**, *117*, 106543. [CrossRef]
52. Wei, W.; Nan, S.; Xie, B.; Liu, C.; Zhou, J.; Liu, C. The Spatial-Temporal Changes of Supply-Demand of Ecosystem Services and Ecological Compensation: A Case Study of Hexi Corridor, Northwest China. *Ecol. Eng.* **2023**, *187*, 106861. [CrossRef]
53. Xiang, H.; Zhang, J.; Mao, D.; Wang, Z.; Qiu, Z.; Yan, H. Identifying Spatial Similarities and Mismatches between Supply and Demand of Ecosystem Services for Sustainable Northeast China. *Ecol. Indic.* **2022**, *134*, 108501. [CrossRef]
54. Li, W.; Wang, Y.; Xie, S.; Cheng, X. Coupling Coordination Analysis and Spatiotemporal Heterogeneity between Urbanization and Ecosystem Health in Chongqing Municipality, China. *Sci. Total Environ.* **2021**, *791*, 148311. [CrossRef] [PubMed]
55. Zhao, J.; Xiao, Y.; Sun, S.; Sang, W.; Axmacher, J.C. Does China's Increasing Coupling of 'Urban Population' and 'Urban Area' Growth Indicators Reflect a Growing Social and Economic Sustainability? *J. Environ. Manag.* **2022**, *301*, 113932. [CrossRef] [PubMed]
56. Shearman, T.M.; Varner, J.M.; Hood, S.M.; Cansler, C.A.; Hiers, J.K. Modelling Post-Fire Tree Mortality: Can Random Forest Improve Discrimination of Imbalanced Data? *Ecol. Model.* **2019**, *414*, 108855. [CrossRef]
57. Xue, C.; Xue, L.; Chen, J.; Tarolli, P.; Chen, X.; Zhang, H.; Qian, J.; Zhou, Y.; Liu, X. Understanding Driving Mechanisms behind the Supply-Demand Pattern of Ecosystem Services for Land-Use Administration: Insights from a Spatially Explicit Analysis. *J. Clean. Prod.* **2023**, *427*, 139239. [CrossRef]
58. Yang, M.; Gao, X.; Zhao, X.; Wu, P. Scale Effect and Spatially Explicit Drivers of Interactions between Ecosystem Services—A Case Study from the Loess Plateau. *Sci. Total Environ.* **2021**, *785*, 147389. [CrossRef]
59. McMillen, D.P. Geographically Weighted Regression: The Analysis of Spatially Varying Relationships. *Am. J. Agric. Econ.* **2004**, *86*, 554–556. [CrossRef]
60. Baró, F.; Gómez-Baggethun, E.; Haase, D. Ecosystem Service Bundles along the Urban-Rural Gradient: Insights for Landscape Planning and Management. *Ecosyst. Serv.* **2017**, *24*, 147–159. [CrossRef]
61. Raudsepp-Hearne, C.; Peterson, G.D.; Bennett, E.M. Ecosystem Service Bundles for Analyzing Tradeoffs in Diverse Landscapes. *Proc. Natl. Acad. Sci. USA* **2010**, *107*, 5242–5247. [CrossRef]
62. Bryan, B.A.; Ye, Y.; Zhang, J.; Connor, J.D. Land-Use Change Impacts on Ecosystem Services Value: Incorporating the Scarcity Effects of Supply and Demand Dynamics. *Ecosyst. Serv.* **2018**, *32*, 144–157. [CrossRef]
63. Deng, C.; Liu, J.; Liu, Y.; Li, Z.; Nie, X.; Hu, X.; Wang, L.; Zhang, Y.; Zhang, G.; Zhu, D.; et al. Spatiotemporal Dislocation of Urbanization and Ecological Construction Increased the Ecosystem Service Supply and Demand Imbalance. *J. Environ. Manag.* **2021**, *288*, 112478. [CrossRef] [PubMed]
64. Ren, Q.; Liu, D.; Liu, Y. Spatio-Temporal Variation of Ecosystem Services and the Response to Urbanization: Evidence Based on Shandong Province of China. *Ecol. Indic.* **2023**, *151*, 110333. [CrossRef]
65. Xu, Q.; Dong, Y.; Yang, R.; Zhang, H.; Wang, C.; Du, Z. Temporal and Spatial Differences in Carbon Emissions in the Pearl River Delta Based on Multi-Resolution Emission Inventory Modeling. *J. Clean. Prod.* **2019**, *214*, 615–622. [CrossRef]
66. Wan, M.; Han, Y.; Song, Y.; Hashimoto, S. Estimating and Projecting the Effects of Urbanization on the Forest Habitat Quality in a Highly Urbanized Area. *Urban For. Urban Green.* **2024**, *94*, 128270. [CrossRef]
67. Han, H.; Guo, L.; Zhang, J.; Zhang, K.; Cui, N. Spatiotemporal Analysis of the Coordination of Economic Development, Resource Utilization, and Environmental Quality in the Beijing-Tianjin-Hebei Urban Agglomeration. *Ecol. Indic.* **2021**, *127*, 107724. [CrossRef]
68. Zhang, X.; Liu, Y.; Wang, Y.; Yuan, X. Interactive Relationship and Zoning Management between County Urbanization and Ecosystem Services in the Loess Plateau. *Ecol. Indic.* **2023**, *156*, 111021. [CrossRef]
69. Yurui, L.; Xuanchang, Z.; Zhi, C.; Zhengjia, L.; Zhi, L.; Yansui, L. Towards the Progress of Ecological Restoration and Economic Development in China's Loess Plateau and Strategy for More Sustainable Development. *Sci. Total Environ.* **2021**, *756*, 143676. [CrossRef] [PubMed]
70. Yan, J.; Liu, D.; Yao, S.; Li, J. An Empirical Study on the Impact of Industrial Structure Change on Environmental Level in China. *Int. J. Econ. Energy Environ.* **2023**, *8*, 82. [CrossRef]
71. Yin, J.; Wang, S.; Gong, L. The Effects of Factor Market Distortion and Technical Innovation on China's Electricity Consumption. *J. Clean. Prod.* **2018**, *188*, 195–202. [CrossRef]
72. Bai, Y.; Liu, W.; Yang, W.; Zuo, W.; Song, H. Urbanization, Industrial Structure Upgrading, and Lottery Consumption Based on the Sustainable Development of the Emerging Markets: Evidence from China. *SAGE Open* **2023**, *13*, 21582440231182323. [CrossRef]
73. Zhong, Y.; Wei, Y.D. Economic Transition, Urban Hierarchy, and Service Industry Growth in China. *Tijdschr.Voor Econ. Soc. Geogr.* **2018**, *109*, 189–209. [CrossRef]

74. Henderson, J.V.; Wang, H.G. Aspects of the Rural-Urban Transformation of Countries. *J. Econ. Geogr.* **2005**, *5*, 23–42. [CrossRef]
75. Shi, L. Changes of Industrial Structure and Economic Growth in Coastal Regions of China: A Threshold Panel Model Based Study. *J. Coast. Res.* **2020**, *107*, 278. [CrossRef]
76. Jung, C.G.; Xu, X.; Niu, S.; Liang, J.; Chen, X.; Shi, Z.; Jiang, L.; Luo, Y. Experimental Warming Amplified Opposite Impacts of Drought vs. Wet Extremes on Ecosystem Carbon Cycle in a Tallgrass Prairie. *Agric. For. Meteorol.* **2019**, *276–277*, 107635. [CrossRef]
77. Underwood, E.C.; Hollander, A.D.; Safford, H.D.; Kim, J.B.; Srivastava, L.; Drapek, R.J. The Impacts of Climate Change on Ecosystem Services in Southern California. *Ecosyst. Serv.* **2019**, *39*, 101008. [CrossRef]
78. Zhang, J.; Zhang, P.; Wang, R.; Liu, Y.; Lu, S. Identifying the Coupling Coordination Relationship between Urbanization and Forest Ecological Security and Its Impact Mechanism: Case Study of the Yangtze River Economic Belt, China. *J. Environ. Manag.* **2023**, *342*, 118327. [CrossRef]

Disclaimer/Publisher's Note: The statements, opinions and data contained in all publications are solely those of the individual author(s) and contributor(s) and not of MDPI and/or the editor(s). MDPI and/or the editor(s) disclaim responsibility for any injury to people or property resulting from any ideas, methods, instructions or products referred to in the content.